Fe and Cu dual-doped Ni_3S_4 nanoarray with less low-valence Ni species for boosting water oxidation reaction

Xiaoqiang Du[a*], Jiaxin Li[a] and Xiaoshuang Zhang[b]

[a]School of Chemical Engineering and Technology, North University of China, Xueyuan road 3, Taiyuan 030051, People's Republic of China. E-mail: duxq16@nuc.edu.cn

[b]School of Science, North University of China, Xueyuan road 3, Taiyuan 030051, People's Republic of China.

DFT calculation

The DFT calculations were performed using the Cambridge Sequential Total Energy Package (CASTEP) with the plane-wave pseudo-potential method. The geometrical structures of the (220) plane of Fe-Cu-Ni_3S_4 were optimized by the generalized gradient approximation (GGA) methods. The Revised Perdew-Burke-Ernzerh of (RPBE) functional was used to treat the electron exchange correlation interactions. A Monkhorst Pack grid k-points of 4*3*1 of Fe-Cu-Ni_3S_4, a plane-wave basis set cut-off energy of 400 eV were used for integration of the Brillouin zone. The structures were optimized for energy and force convergence set at 0.05 eV/A and 2.0×10^{-5} eV, respectively. The vacuum space was up to 0.002 A to eliminate periodic interactions.

Table S1. ICP data of Fe-Cu-Ni_3S_4 nanosheets.

element	atomic percentage(At %)
Fe	4.08
Cu	4.61
Ni	36.51
S	45.37

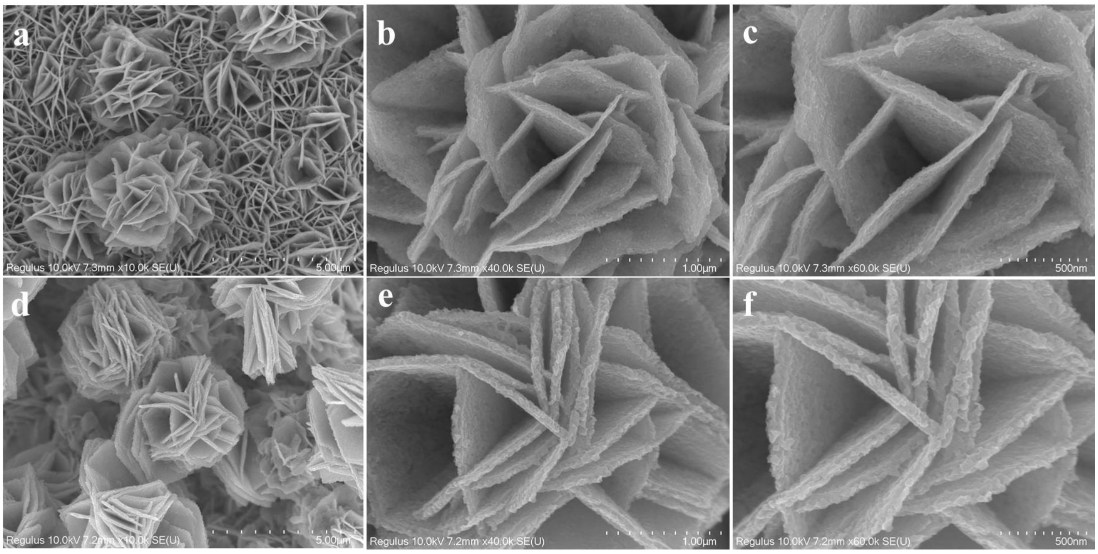

Fig. S1. SEM images of Fe-Ni_3S_4 with (a) low and (b,c) high magnifications. SEM images of Cu-Ni_3S_4 with (d) low and (e,f) high magnifications.

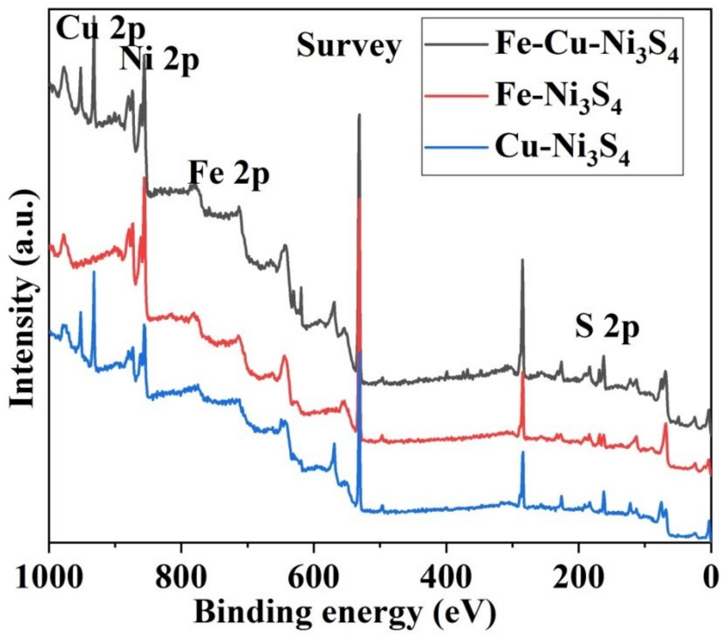

Fig. S2. XPS survey spectrum for Fe-Ni_3S_4, Cu-Ni_3S_4 and Fe-Cu-Ni_3S_4 nanosheets.

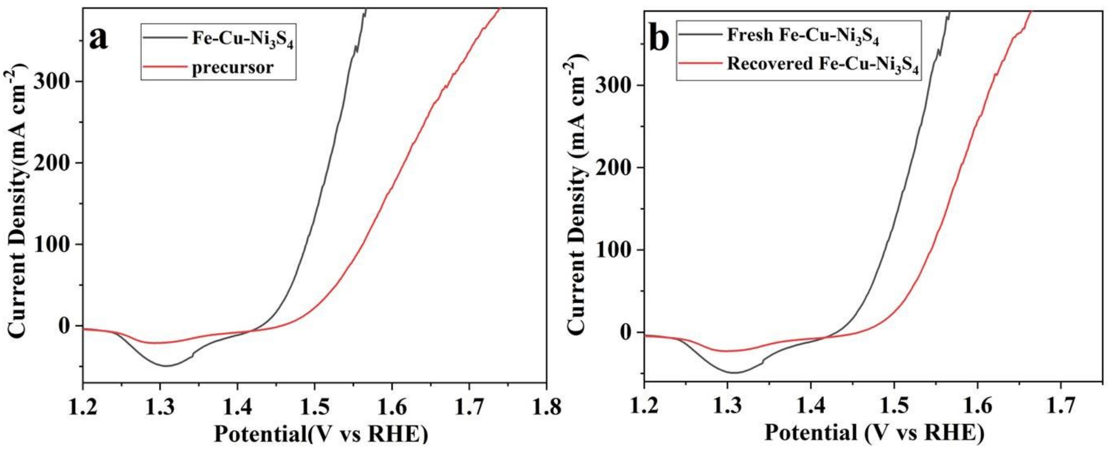

Fig. S3. (a) Linear sweep voltammetry polarization curves of the precursor and Fe-Cu-Ni_3S_4. (b) Linear sweep voltammetry polarization curves of Fe-Cu-Ni_3S_4 before and after 10 h.

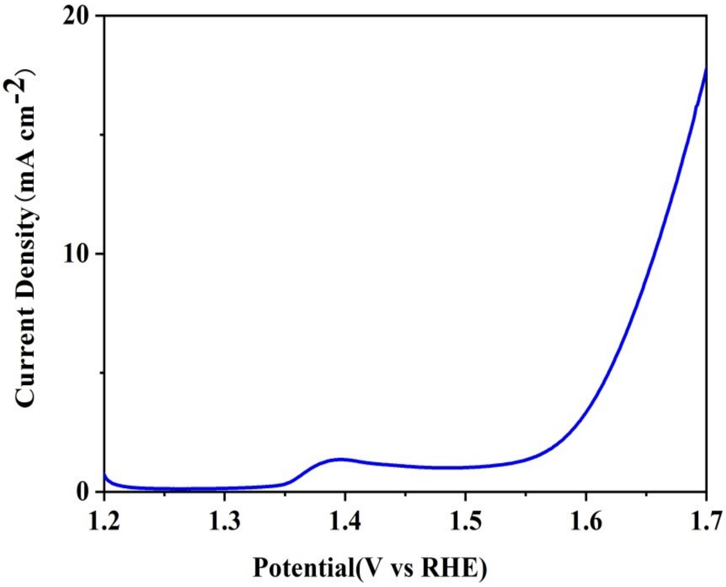

Fig. S4 Polarization curve of the Ni foam for OER with a scan rate of 5 mV s^{-1} in 1 M KOH.

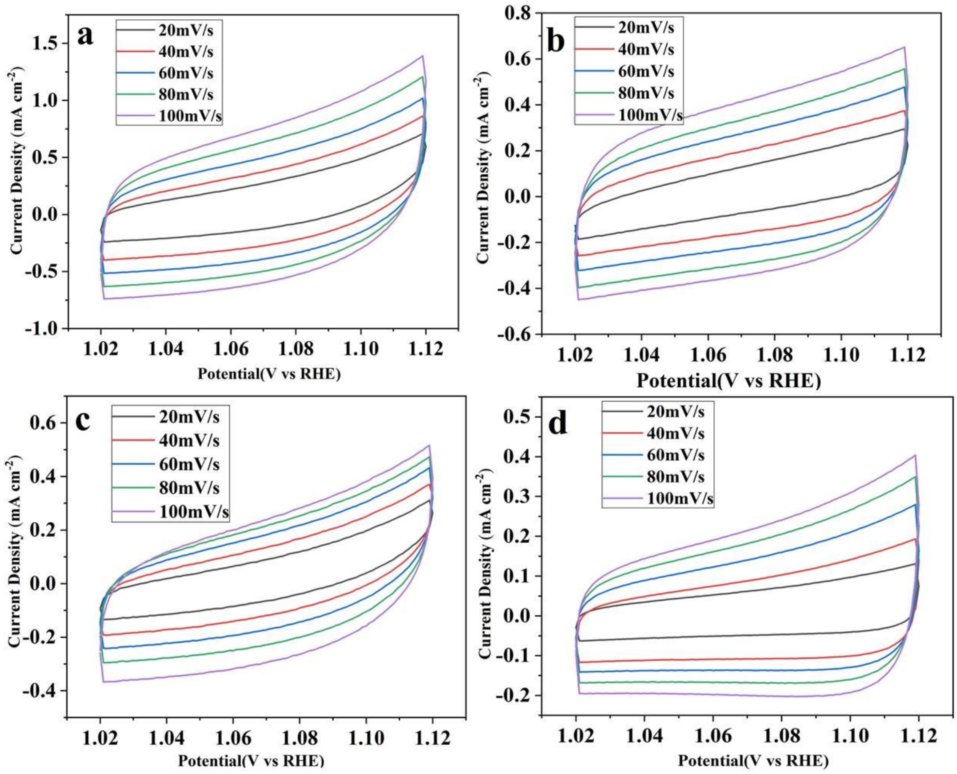

Fig. S5 CV curves with different scan rates in OER,Fe-Cu-Ni_3S_4/NF (a), Fe-Ni_3S_4/NF (b), Cu-Ni_3S_4/NF (c) Ni_3S_4/NF (d).

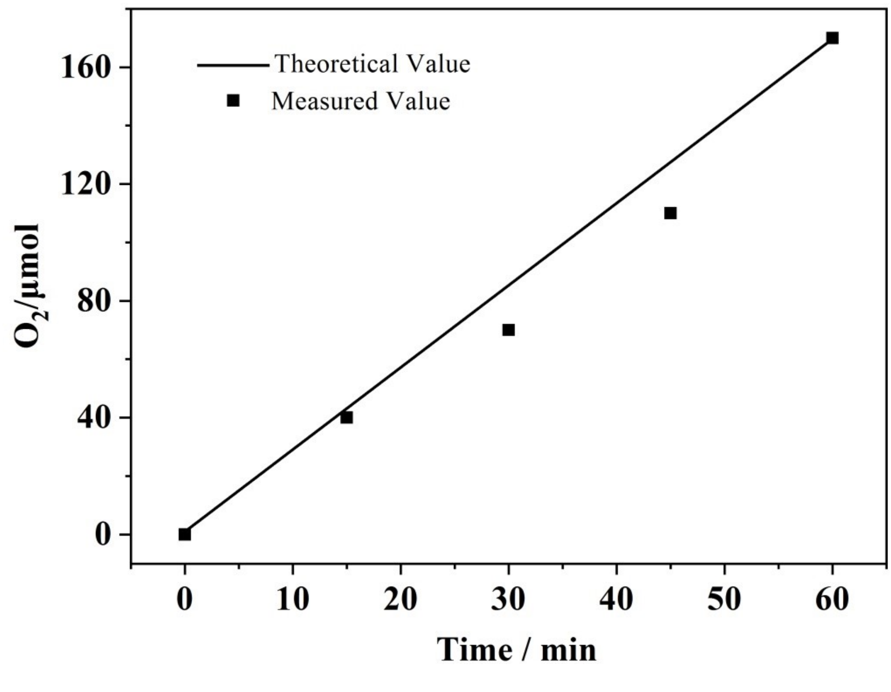

Fig. S6 Electrocatalytic efficiency of O_2 production over Fe-Cu-Ni_3S_4/NF.

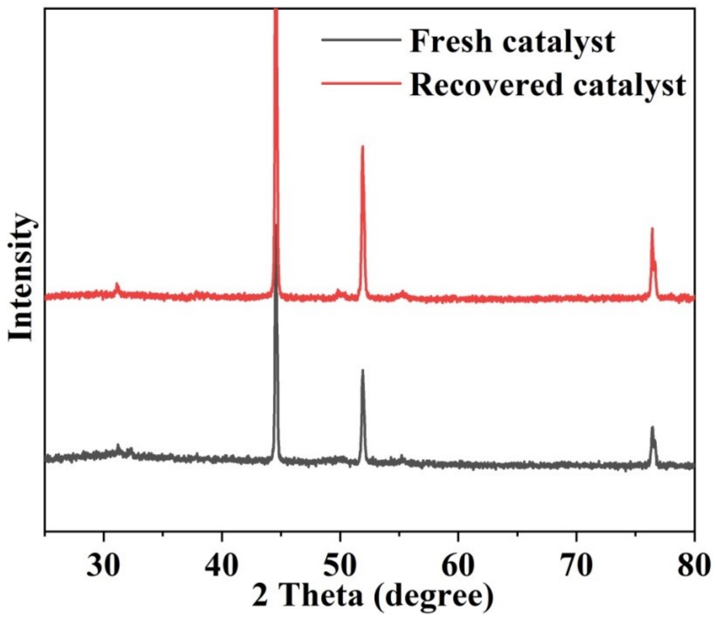

Fig. S7 XRD of fresh and recovered Fe-Cu-Ni_3S_4/NF after OER.

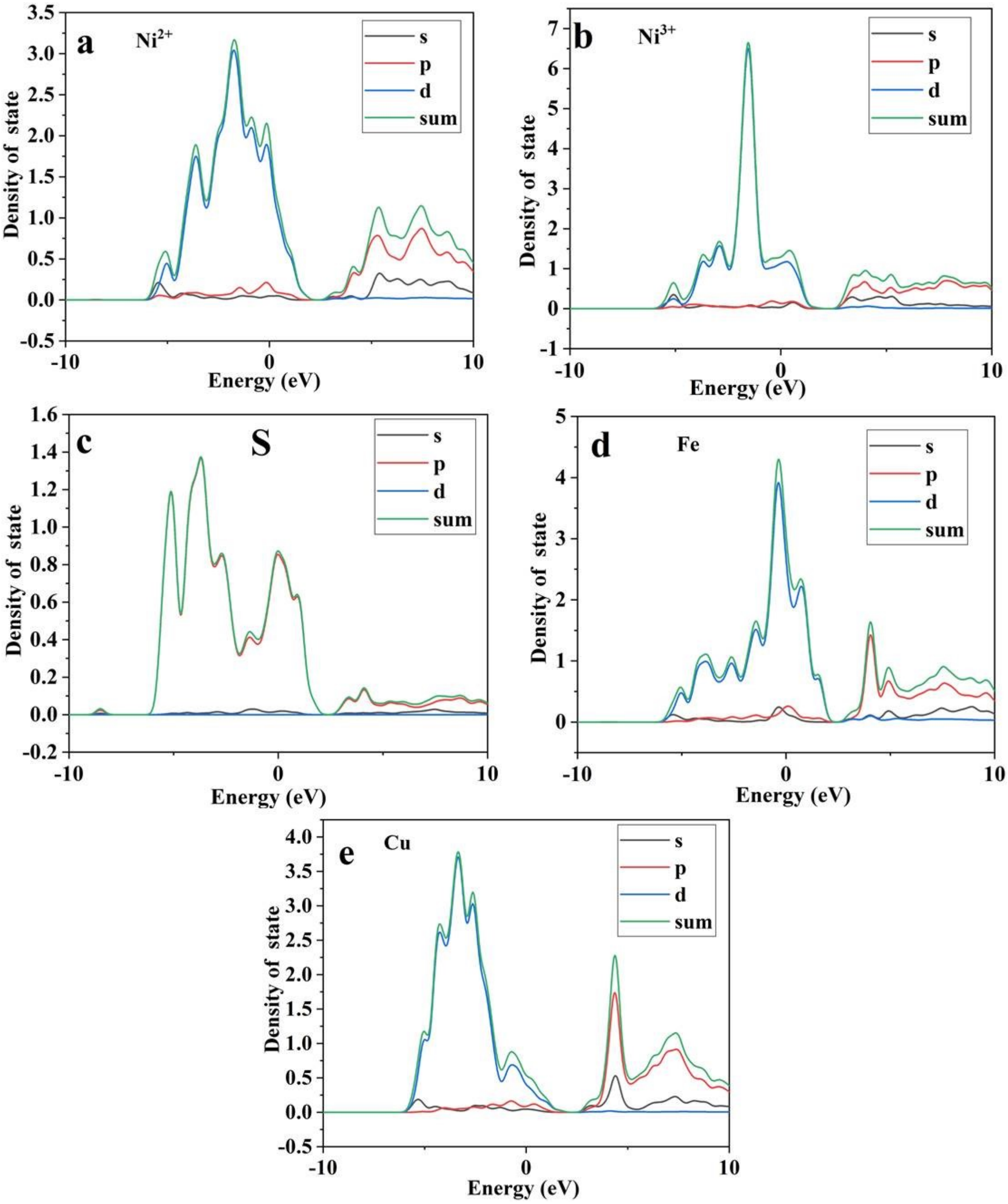

Fig. S8 Density of states (Ni^{2+} as adsorption sites) for Fe-Cu-Ni_3S_4, (a) Ni^{2+}, (b) Ni^{3+}, (c) S, (d) Fe and (e) Cu.

Table S2. Comparison of recently reported catalytic properties of element doped Nickel based sulfides.

Electrocatalysts	Overpotential	References
Fe-Cu-Ni_3S_4	**230 mV at 50 mA cm^{-2}**	**This work**
FeCo-Ni_3S_4	230 mV at 20 mA cm^{-2}	Chem. Eng. J. 2022, 427, 130742
N doped NiS_2 nanoarrays	270 mV at 10 mA cm^{-2}	J. Mater. Chem. A, 2017, 5, 17811–17816
Ni^{3+} self-doped Ni_3S_4	266 mV at 10 mA cm^{-2}	J.Colloid Interf. Sci. 2020,564, 418–427
Co and Ce dual doped Ni_3S_2	280 mV at 20 mA cm^{-2}	Nano Res. 2020,13, 2130–2135
Cu and Co co-doped Ni_3S_2	370 mV at 10 mA cm^{-2}	Appl. Sur. Sci. 2020,502, 144172
Fe-doped Ni_3S_2	295 mV at 10 mA cm^{-2}	Nanoscale, 2019, 11, 2355
N-doped Ni-Ni_3S_2@carbon nanoplates	284 mV at 10 mA cm^{-2}	Small 2019, 15, 1900348
Cu-doped Ni_3S_2	259 mV at 10 mA cm^{-2}	J. Solid State Chem. 2021,293, 121776

Table S3. Comparison of recently reported catalytic properties of nickel based sulfides.

Electrocatalysts	Overpotential	References
Fe-Cu-Ni_3S_4	**230 mV at 50 mA cm^{-2}**	**This work**
Ni_3S_2	296 mV at 10 mA cm^{-2}	J. Mater. Chem. A, 2019, 7, 18003–18011
NiS/C_3N_4	334 mV at 10 mA cm^{-2}	Chem. Eng. J. 2021, 410, 128394
Ni_3S_2/NiS	298 mV at 10 mA cm^{-2}	ACS Appl. Mater. Interfaces 2019, 11, 26, 23180–23191
Ni_3S_2 superstructures	340 mV at 10 mA cm^{-2}	J. Mater. Chem. A, 2016, 4, 13916–13922
NiS/NiS_2	416 mV at 100 mA cm^{-2}	J. Mater. Chem. A, 2018, 6, 8233–8237
MoS_2/NiS	350 mV at 10 mA cm^{-2}	Small 2019, 15, 1803639
NiS_2/CoS_2 nanowires	235 mV at 10 mA cm^{-2}	Adv. Mater. 2017, 29, 1704681
porous Ni_3S_4	257 mV at 10 mA cm^{-2}	Adv. Funct. Mater. 2019, 29, 1900315
Ni_3S_4/N,P-C	370 mV at 10 mA cm^{-2}	Chem. Eur. J. 2019, 25, 7561 – 7568
Ni_3S_2 nanosheet	260 mV at 10 mA cm^{-2}	J. Am. Chem. Soc. 2015, 137, 14023−14026

Table S4. Comparison of OER performances for Fe-Cu-Ni_3S_4 with other reported electrocatalysts.

Electrocatalysts	Overpotential	References
Fe-Cu-Ni_3S_4	**230 mV at 50mA cm^{-2}**	**This work**
CoO_x/FeO_x/CNT	308 mV at 10 mA cm^{-2}	J. Mater. Chem. A, 2020, 8, 15140–15147
NiS_2/$NiSe_2$ nanocage	290 mV at 20 mA cm^{-2}	Small 2020, 16, 1905083
Co-Fe-V metal oxides	249 mV at 10 mA cm^{-2}	J. Mater. Chem. A, 2020, 8, 15951–15961
P-doped $NiCo_2O_4$	300 mV at 10 mA cm^{-2}	ACS Appl. Mater. Interfaces 2020, 12, 2763−2772
NiS/Fe_3O_4 HNPs@CNT	243 mV at 10 mA cm^{-2}	ACS Appl. Mater. Interfaces 2020, 12, 31552−31563
Fe_3O_4/FeS_2	253 mV at 10 mA cm^{-2}	J. Mater. Chem. A, 2020, 8, 14145–14151
CoMoOS nanoboxes	281 mV at 10 mA cm^{-2}	Appl. Catal. B: Environ. 2020, 265, 118605
$Ni_{59}Cu_{19}P_9$	307 mV at 10 mA cm^{-2}	Appl. Catal. B: Environ. 2018, 237, 409–415
Fe-Ni-P-B-O	236 mV at 10 mA cm^{-2}	ACS Nano 2019, 13, 12969−12979
hollow Fe-Co_xP	300 mV at 10 mA cm^{-2}	Chem. Eng. J. 2021, 409, 128227